

Simple Description of $\pi\pi$ Scattering to 1 GeV

Masayasu Harada^{a*}, *Francesco Sannino*^{a,b †}

and

Joseph Schechter^{a ‡}

^a *Department of Physics, Syracuse University, Syracuse, New York, 13244-1130.*

^b *Dipartimento di Scienze Fisiche, Mostra d'Oltremare Pad.19, 80125 Napoli, Italia.*

Abstract

Motivated by the $1/N_c$ expansion, we present a simple model of $\pi\pi$ scattering as a sum of a *current-algebra* contact term and resonant pole exchanges. The model preserves crossing symmetry as well as unitarity up to 1.2 GeV. Key features include chiral dynamics, vector meson dominance, a broad low energy scalar (σ) meson and a *Ramsauer-Townsend* mechanism for the understanding of the 980 MeV region. We discuss in detail the *regularization* (corresponding to rescattering effects) necessary to make all these nice features work.

**e-mail:* mharada@npac.syr.edu

†*e-mail:* sannino@npac.syr.edu

‡*e-mail:* schechter@suhep.phy.syr.edu

1 Introduction

Historically, the analysis of $\pi\pi$ scattering has been considered an important test of our understanding of strong interaction physics (QCD, now) at low energies. It is commonly accepted that the key feature is the approximate spontaneous breaking of chiral symmetry. Of course, the *kinematical* requirements of unitarity and crossing symmetry should be respected. The chiral perturbation scheme [1], which improves the tree Lagrangian approach by including loop corrections and counterterms, can provide a description of the scattering up to the energy region slightly above threshold ($400 - 500 \text{ MeV}$).

In order to describe the scattering up to energies beyond this region (say to around 1 GeV) it is clear that the effects of particles lying in this region must be included and some new principle invoked. A plausible hint comes from the large N_c approximation to QCD, in which the leading order scattering amplitudes consist of just tree diagrams containing resonance exchanges as well as possible contact diagrams [2]. The method suggests that an infinite number of resonances are required and also a connection with some kind of string theory [3].

Some encouraging features were previously found in an approach which truncated the particles appearing in the effective Lagrangian to those with masses up to an energy slightly greater than the range of interest. This seems reasonable phenomenologically and is what one usually does in setting up an effective Lagrangian. The most famous example is the chiral Lagrangian of only pions. In Ref. [4] this Lagrangian provided, as a starting point, a contact term which described the threshold region. However the usual observation was made that the real part of the $I = 0, J = 0$ partial wave amplitude quite soon violated the unitarity bound $|R_0^0| \leq 1/2$ rather severely. The inclusion of the contribution coming from the ρ meson exchange was observed to greatly improve, although not completely solve, this problem. These results are shown explicitly in Fig. 1 and provide some encouragement for the possible success of a truncation scheme.

In Ref. [4], it was observed that the inclusion of resonances up till and including the p -wave region enabled one to construct an amplitude which satisfied the unitarity bounds up to about 1.3 GeV . It was assumed that, above this point, new resonances would come

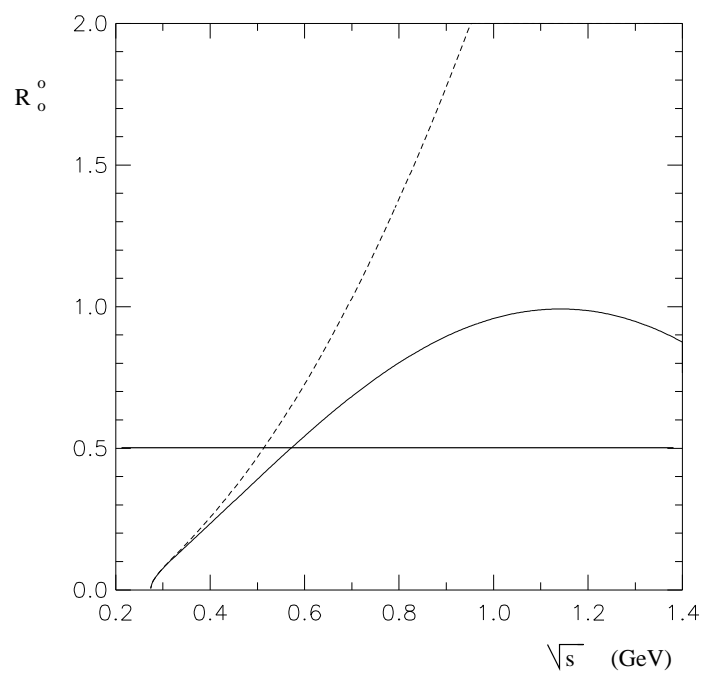


Figure 1: Predicted curves for R_0^0 . The solid line which shows the *current algebra* + ρ result for R_0^0 is much closer to the unitarity bound of 0.5 than the dashed line which shows the *current algebra* result alone.

in to preserve unitarity. This hypothesis was called *local cancellation*. The model produced a reasonable looking $I = J = 0$ phase shift up to about 800 MeV . In this paper we will attempt to describe and carefully compare with experiment the interesting physics lying between 800 and 1200 MeV in this truncated $1/N_c$ inspired framework. Specifically we will be concerned with the proper inclusion of the $f_0(980)$ scalar resonance as well as the opening of the $K\bar{K}$ channel. We find that a simple reasonable description of the $f_0(980)$ region is obtained when the interplay of this resonance with its background is taken into account. In this approach the background amplitude is predicted by the model itself. In the region just above the $K\bar{K}$ threshold we notice the feature analogous to the elastic case that the severe unitarity violation of the inelastic $\pi\pi \rightarrow K\bar{K}$ amplitude is damped by the inclusion of vector meson and scalar meson exchange diagrams.

Of course, it would be wonderful if one could simply add the various contributions to the tree level amplitude and find a good match to experiment. This is not possible for a variety of reasons, which are discussed in Section 2. The needed *regularizations* are introduced there. Section 3 gives a brief overview of the model and reviews the important role of a broad scalar meson in the low energy ($< 800 \text{ MeV}$) region. Section 4 contains a discussion of various aspects of the 1 GeV region. The characteristic feature - a type of *Ramsauer-Townsend* effect resulting from the interplay of the $f_0(980)$ resonance with the predicted background - is outlined in section 4.1 and treated in more detail in 4.2. In section 4.3 it is shown that the introduction of the *next group* of resonances, located in the 1300 MeV region, does not make major changes in the $\pi\pi$ scattering below 1200 MeV (the changes are essentially absorbed in small changes of the parameters of the broad low energy scalar). In section 4.4 it is demonstrated that the phenomenological introduction of inelastic effects associated with the opening of the $K\bar{K}$ channel does not make a significant change in our picture of $\pi\pi \rightarrow \pi\pi$ below 1200 MeV . Section 4.5 contains a presentation of the $I = J = 0$ phase shift obtained by combining our predicted real part with unitarity. In section 5 we discuss the inelastic $\pi\pi \rightarrow K\bar{K}$ channel and show that here also the resonance exchanges damp the unitarity bound violation due to the contact term. Section 6 contains the summary and further discussion. Finally, Appendices A, B and C give details on, respectively, the scattering kinematics, the chiral Lagrangian and the unregularized amplitudes.

2 Difficulties of the Approach

In the large N_c picture the leading amplitude (of order $1/N_c$) is a sum of polynomial contact terms and tree type resonance exchanges. Furthermore the resonances should be of the simple $q\bar{q}$ type; glueball and multi-quark meson resonances are suppressed. In our phenomenological model there is no way of knowing *a priori* whether a given experimental state is actually of $q\bar{q}$ type. For definiteness we will keep all relevant resonances even though the status of a low lying scalar resonance like the $f_0(980)$ has been considered especially controversial [5]. If such resonances turn out in the future to be not of $q\bar{q}$ type, their tree contributions would be of higher order than $1/N_c$. In this event the amplitude would still of course satisfy crossing symmetry.

The most problematic feature involved in comparing the leading $1/N_c$ amplitude with experiment is that it does not satisfy unitarity. In fact, resonance poles like

$$\frac{1}{M^2 - s} \tag{2.1}$$

will yield a purely real amplitude, except at the singularity, where they will diverge and drastically violate the unitarity bound. Thus in order to compare the $1/N_c$ amplitude with experiment we must regularize the denominators in some way. The usual method, as employed in Ref. [4], is to regularize the propagator so that the resulting partial wave amplitude has the locally unitary form

$$\frac{M\Gamma}{M^2 - s - iM\Gamma} . \tag{2.2}$$

This is only valid for a narrow resonance in a region where the *background* is negligible. Note that the $-iM\Gamma$ is strictly speaking a higher order in $1/N_c$ effect.

For a very broad resonance there is no guarantee that such a form is correct. Actually, in Ref. [4] it was found necessary to include a rather broad low lying scalar resonance (denoted $\sigma(550)$) to avoid violating the unitarity bound. A suitable form turned out to be of the type

$$\frac{MG}{M^2 - s - iMG'} , \tag{2.3}$$

where G is not equal to the parameter G' which was introduced to regularize the propagator. Here G is the quantity related to the squared coupling constant.

Even if the resonance is narrow, the effect of the background may be rather important. This seems to be true for the case of the $f_0(980)$. Demanding local unitarity in this case yields a partial wave amplitude of the well known form [6]:

$$\frac{e^{2i\delta} M\Gamma}{M^2 - s - iM\Gamma} + e^{i\delta} \sin \delta , \quad (2.4)$$

where δ is a background phase (assumed to be slowly varying). We will adopt a point of view in which this form is regarded as a kind of regularization of our model. Of course, non zero δ represents a rescattering effect which is of higher order in $1/N_c$. The quantity $e^{2i\delta}$, taking $\delta = \text{constant}$, can be incorporated into the squared coupling constant connecting the resonance to two pions. In this way, crossing symmetry can be preserved. From its origin, it is clear that the complex residue does not signify the existence of a *ghost* particle. The non-pole background term in eq. (2.4) and hence δ is to be predicted by the other pieces in the effective Lagrangian.

Another point which must be addressed in comparing the leading $1/N_c$ amplitude with experiment is that it is purely real away from the singularities. The regularizations mentioned above do introduce some imaginary pieces but these are clearly more model dependent. Thus it seems reasonable to compare the real part of our predicted amplitude with the real part of the experimental amplitude. Note that the difficulties mentioned above arise only for the direct channel poles; the crossed channel poles and contact terms will give purely real finite contributions.

It should be noted that if we predict the real part of the amplitude, the imaginary part can always be recovered by assuming elastic unitarity (which is likely to be a reasonable approximation up to about 1 GeV). Specializing eq. (A.6) in Appendix A to the $\pi\pi$ channel we have for the imaginary piece I_l^I of the I , l partial wave amplitude

$$I_l^I = \frac{1}{2} \left[1 \pm \sqrt{\eta_l^{I^2} - 4R_l^{I^2}} \right] , \quad (2.5)$$

where η_l^I is the elasticity parameter. Obviously this formula is only meaningful if the real part obeys the bound

$$|R_l^I| \leq \frac{\eta_l^I}{2} . \quad (2.6)$$

The main difficulty one has to overcome in obtaining a unitary amplitude by the present method is the satisfaction of this bound. Therefore, one sees that making *regularizations* like

	$I^G(J^{PC})$	$M(\text{MeV})$	$\Gamma_{tot}(\text{MeV})$	$Br(2\pi)\%$
$\sigma(550)$	$0^+(0^{++})$	559	370	–
$\rho(770)$	$1^+(1^{--})$	769.9	151.2	100
$f_0(980)$	$0^+(0^{++})$	980	40–400	78.1
$f_2(1270)$	$0^+(2^{++})$	1275	185	84.9
$f_0(1300)$	$0^+(0^{++})$	1000-1500	150–400	93.6
$\rho(1450)$	$1^+(1^{--})$	1465	310	seen

Table 1: Resonances included in the $\pi\pi \rightarrow \pi\pi$ channel as listed in the PDG. Note that the σ is not present in the PDG and is not being described exactly as a *Breit-Wigner* shape; we listed the fitted parameters shown in column 1 of Table 2 where G' is the analog of the *Breit-Wigner* width.

eqs. (2.2) and (2.4) which provide unitarity in the immediate region of a narrow resonance is not at all tantamount to unitarizing the model by hand. One might glance again at Fig. 1 for emphasis of this point.

To summarize this discussion, we will proceed by comparing the real part of a suitably regularized tree amplitude computed from a chiral Lagrangian of pseudoscalar mesons and resonances with the real part of the experimental amplitude deduced from the standard phase shift analysis.

3 Overview and Low Energy Region

The amplitude will be constructed from the non-linear chiral Lagrangian briefly summarized in Appendix B. To start with, we shall neglect the existence of the K mesons. Then the form of the unregularized amplitude is identical to the one presented in Ref. [4]. The neutral resonances which can contribute have the quantum numbers $J^{PC} = 0^{++}$, 1^{--} , and 2^{++} . We show in Table 1 the specific ones which are included, together with their masses and widths, when available from the Particle Data Group (PDG) [7] listings.

Essentially there are only three arbitrary parameters in the whole model, these correspond to the three unknowns in the description of a broad scalar resonance given by eq. (2.3). We will include only the minimal two derivative chiral contact interaction contained in eq. (B.7)

of Appendix B. Clearly, higher derivative contact interaction may also be included (see, for example, sec. III.E of Ref. [4]).

As shown in Fig. 1, although the introduction of the ρ dramatically improves unitarity up to about 2 GeV, R_0^0 violates unitarity to a lesser extent starting around 500 MeV. (As noted in Ref. [4], the $I = J = 0$ channel is the only troublesome one.) To completely restore unitarity in the present framework it is necessary to include a low mass broad scalar state which has historically been denoted as the σ . It seems helpful to recall the contribution of such a particle to the real part of the amplitude component $A(s, t, u)$ defined in eq. (A.8):

$$\text{Re}A_\sigma(s, t, u) = \text{Re} \frac{32\pi}{3H} \frac{G}{M_\sigma^3} (s - 2m_\pi^2)^2 \frac{(M_\sigma^2 - s) + iM_\sigma G'}{(s - M_\sigma^2)^2 + M_\sigma^2 G'^2}, \quad (3.1)$$

where

$$H = \left(1 - 4\frac{m_\pi^2}{M_\sigma^2}\right)^{\frac{1}{2}} \left(1 - 2\frac{m_\pi^2}{M_\sigma^2}\right)^2 \approx 1, \quad (3.2)$$

and G is related to the coupling constant γ_0 defined in eq. (B.11) by

$$G = \gamma_0^2 \frac{3HM_\sigma^3}{64\pi}. \quad (3.3)$$

Note that the factor $(s - 2m_\pi^2)^2$ is due to the derivative-type coupling required for chiral symmetry in eq. (B.11). The total amplitude will be crossing symmetric since $A(s, t, u)$ and $A(u, t, s)$ in eq. (A.8) are obtained by performing the indicated permutations. G' is a parameter which we introduce to regularize the propagator. It can be called a width, but it turns out to be rather large so that, after the ρ and π contributions are taken into account, the partial wave amplitude R_0^0 does not clearly display the characteristic resonant behavior. In the most general situation one might imagine that G could become complex as in eq. (2.4) due to higher order in $1/N_c$ corrections. It should be noted, however, that eq. (2.4) expresses nothing more than the assumption of unitarity for a *narrow* resonance and hence should not really be applied to the present broad case. A reasonable fit was found in Ref. [4] for G purely real, but not equal to G' . By the use of eq. (2.5), unitarity is in fact locally satisfied.

A best overall fit is obtained with the parameter choices; $M_\sigma = 559$ MeV, $G/G' = 0.29$ and $G' = 370$ MeV. These have been slightly fine-tuned from the values in Ref. [4] in order to obtain a better fit in the 1 GeV region. The result for the real part R_0^0 due to the inclusion of the σ contribution along with the π and ρ contributions is shown in Fig. 2. It is seen that

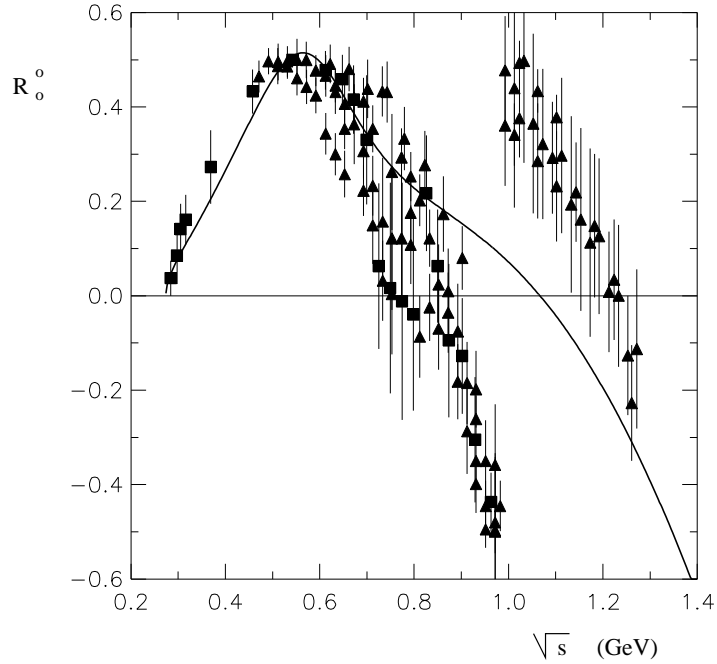


Figure 2: The solid line is the *current algebra* + ρ + σ result for R_0^0 . The experimental points, in this and succeeding figures, are extracted from the phase shifts using eq. (A.6) and actually correspond to R_0^0/η_0^0 . (\square) are extracted from the data of Ref. [8] while (\triangle) are extracted from the data of Ref. [9]. The predicted R_0^0 is small around the 1 *GeV* region.

the unitarity bound is satisfied and there is a reasonable agreement with the experimental points [8, 9] up to about 800 MeV . Beyond this point the effects of other resonances (mainly the $f_0(980)$) are required. From eqs. (3.1), (A.9) and (A.11) we see that the contribution of σ to R_0^0 turns negative when $s > M_\sigma^2$. This is the mechanism which leads to satisfaction of the unitarity bound (c.f. Fig. 1). For $s < M_\sigma^2$ one gets a positive contribution to R_0^0 . This is helpful to push the predicted curve upwards and closer to the experimental results in this region, as shown in Fig. 3. The four-derivative contribution in the chiral perturbation

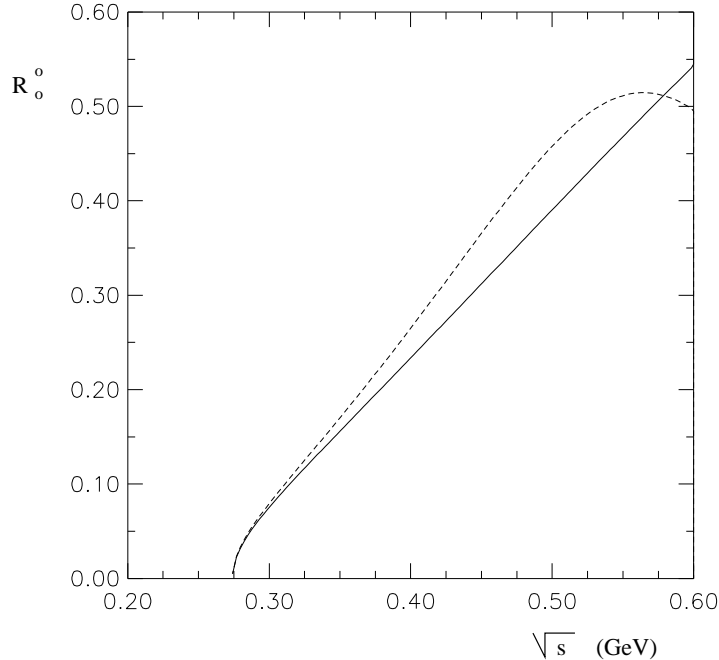


Figure 3: A blowup of the low energy region. The solid line is the *current algebra* + ρ contribution to R_0^0 . The dashed line includes the σ and has the effect of turning the curve down to avoid unitarity violation while boosting it at lower energies.

theory approach performs the same function; however it does not change sign and hence does not satisfy the unitarity bound above the 450 MeV region [10].

4 The 1 GeV Region

4.1 The main point

Reference to Fig. 2 shows that the experimental data for R_0^0 lie considerably lower than the $\pi + \rho + \sigma$ contribution between 0.9 and 1.0 GeV and then quickly reverse sign above this point. We will now see that this distinctive shape is almost completely explained by the inclusion of the relatively narrow scalar resonance $f_0(980)$ in a suitable manner. One can understand what is going on very simply by starting from the real part of eq. (2.4):

$$M\Gamma \frac{(M^2 - s) \cos(2\delta) - M\Gamma \sin(2\delta)}{(M^2 - s)^2 + M^2\Gamma^2} + \frac{1}{2} \sin(2\delta) . \quad (4.1)$$

This expresses nothing more than the restriction of local unitarity in the case of a narrow resonance in the presence of a background. We have seen that the difficulty of comparing the tree level $1/N_c$ amplitude to experiment is enhanced in the neighborhood of a direct channel pole. Hence it is probably most reliable to identify the background term $\frac{1}{2} \sin(2\delta)$ with our prediction for R_0^0 . In the region of interest, Fig. 2 shows that R_0^0 is very small so that one expects, δ to be roughly 90° (assuming a monotonically increasing phase shift). Hence the first, pole term is approximately

$$- \frac{(M^2 - s)M\Gamma}{(M^2 - s)^2 + M^2\Gamma^2} , \quad (4.2)$$

which contains a crucial reversal of sign compared to the real part of eq. (2.2). Thus, just below the resonance there is a sudden *negative* contribution which jumps to a positive one above the resonance. This is clearly exactly what is needed to bring experiment and theory into agreement up till about 1.2 GeV, as is shown in Fig. 4. The actual amplitude used for this calculation properly contains the effects of the pions' derivative coupling to the $f_0(980)$ as in eq. (3.1).

It is interesting to contrast this picture with Fig. 10 in Ref. [4]. There the interaction with the background was not taken into account and there was no reversal of sign. Thus, although the unitarity bound was obeyed, the experimental phase shifts could only be properly predicted up to about 0.8 GeV. If the $f_0(980)$ contribution in that Fig. 10 is flipped in sign it is seen to agree with the present Fig. 4.

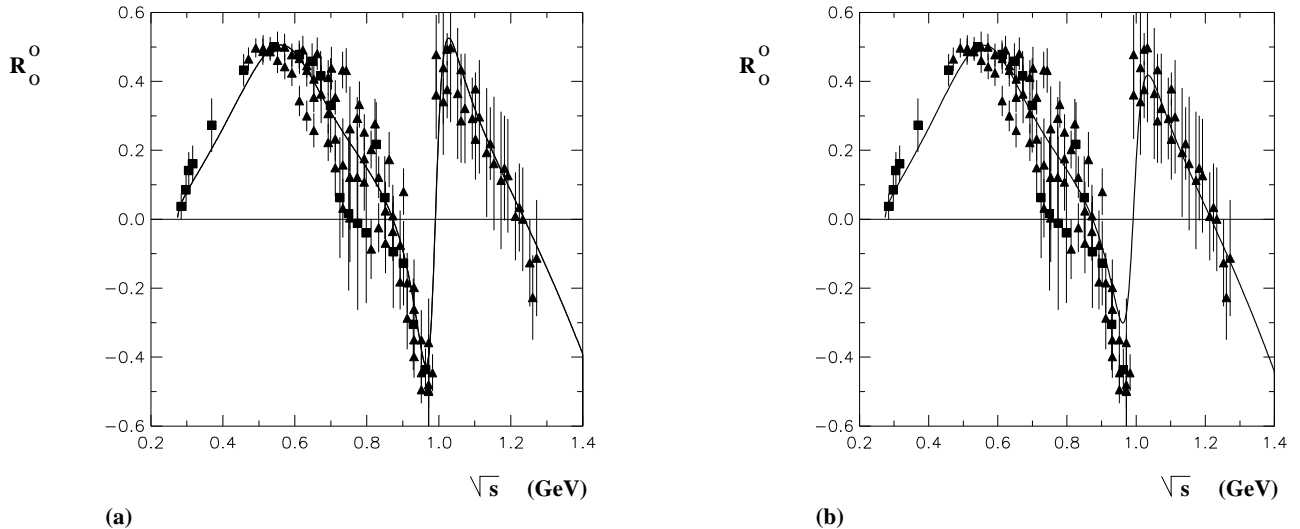


Figure 4: (a): The solid line is the *current algebra* + ρ + σ + $f_0(980)$ result for R_0^0 obtained by assuming column 1 in Table 2 for the σ and $f_0(980)$ parameters ($Br(f_0(980) \rightarrow 2\pi) = 100\%$). (b): The solid line is the *current algebra* + ρ + σ + $f_0(980)$ result for R_0^0 obtained by assuming column 2 in Table 2 ($Br(f_0(980) \rightarrow 2\pi) = 78.1\%$).

The above mechanism, which leads to a sharp dip in the $I = J = 0$ partial wave contribution to the $\pi\pi$ -scattering cross section, can be identified with the very old *Ramsauer-Townsend* effect [11] which concerned the scattering of 0.7 eV electrons on rare gas atoms. The dip occurs because the background phase of $\pi/2$ causes the phase shift to go through π (rather than $\pi/2$) at the resonance position. (Of, course, the cross section is proportional to $\sum_{I,J}(2J+1)\sin^2(\delta_I^J)$.) This simple mechanism seems to be all that is required to understand the main feature of $\pi\pi$ scattering in the 1 GeV region.

4.2 Detailed analysis

Here we will compare with experimental data, the real part of the $I = J = 0$ partial wave amplitude which results from our crossing symmetric model. First we will consider the sum of the contributions of the *current algebra*, ρ -meson, σ and $f_0(980)$ pieces. Then we will add pieces corresponding to the *next group* of resonances; namely, the $f_2(1270)$, the $\rho(1450)$ and the $f_0(1300)$. In this section we will continue to neglect the $K\bar{K}$ channel.

The current algebra plus ρ contribution to the quantity $A(s, t, u)$ defined in eq. (A.8) is[§]

$$\begin{aligned}
A_{ca+\rho}(s, t, u) &= 2\frac{s - m_\pi^2}{F_\pi^2} + \frac{g_{\rho\pi\pi}^2}{2m_\rho^2}(4m_\pi^2 - 3s) + \\
&- \frac{g_{\rho\pi\pi}^2}{2} \left[\frac{u - s}{(m_\rho^2 - t) - im_\rho\Gamma_\rho\theta(t - 4m_\pi^2)} \right. \\
&\left. + \frac{t - s}{(m_\rho^2 - u) - im_\rho\Gamma_\rho\theta(u - 4m_\pi^2)} \right]. \tag{4.3}
\end{aligned}$$

Note that for the $I = J = 0$ channel this will yield a purely real contribution to the partial wave amplitude. The contribution of the low lying σ meson was given in eq. (3.1). For the important $f_0(980)$ piece we have

$$\text{Re}A_{f_0(980)}(s, t, u) = \text{Re} \left[\frac{\gamma_{f_0\pi\pi}^2 e^{2i\delta} (s - 2m_\pi^2)^2}{m_{f_0}^2 - s - im_{f_0}\Gamma_{tot}(f_0)\theta(s - 4m_\pi^2)} \right], \tag{4.4}$$

where δ is a background phase parameter and the real coupling constant $\gamma_{f_0\pi\pi}$ is related to the $f_0(980) \rightarrow \pi\pi$ width by

$$\Gamma(f_0(980) \rightarrow \pi\pi) = \frac{3}{32\pi} \frac{\gamma_{f_0\pi\pi}^2}{m_{f_0}} \sqrt{1 - \frac{4m_\pi^2}{m_{f_0}^2}}. \tag{4.5}$$

We will not consider δ to be a new parameter but shall predict it as

$$\frac{1}{2} \sin(2\delta) \equiv \tilde{R}_0^0(s = m_{f_0}^2), \tag{4.6}$$

where \tilde{R}_0^0 is computed as the sum of the current algebra, ρ , and sigma pieces. Since the $K\bar{K}$ channel is being neglected, one might want to set the *regularization parameter* $\Gamma_{tot}(f_0)$ in the denominator to $\Gamma(f_0(980) \rightarrow \pi\pi)$. We shall try both this possibility as well as the experimental one $\frac{\Gamma(f_0(980) \rightarrow \pi\pi)}{\Gamma_{tot}(f_0)} \approx 78.1\%$.

A best fit of our parameters to the experimental data results in the curves shown in Fig. 4 for both choices of branching ratio. Only the three parameters G/G' , G' and M_σ are essentially free. The others are restricted by experiment. Unfortunately the total width $\Gamma_{tot}(f_0)$ has a large uncertainty; it is claimed by the PDG to lie in the $40 - 400 \text{ MeV}$ range. Hence this is effectively a new parameter. In addition we have considered the precise value of m_{f_0} to be a parameter for fitting purposes. The parameter values for each fit are given in

[§]We introduced the step function $\theta(s - 4m_\pi^2)$ in the propagator and have checked that its inclusion does not make much difference in the results.

					With Next Group				No $\rho(1450)$
$BR(f_0(980) \rightarrow 2\pi)\%$	100	78.1	78.1	78.1	100	78.1	78.1	78.1	100
η_0^0	1	1	0.8	0.6	1	1	0.8	0.6	1
$M_{f_0(980)} (MeV)$	987	989	990	993	991	992	993	998	992
$\Gamma_{tot} (MeV)$	64.6	77.1	75.9	76.8	66.7	77.2	78.0	84.0	64.6
$M_\sigma (MeV)$	559	557	557	556	537	537	535	533	525
$G' (MeV)$	370	371	380	395	422	412	426	451	467
G/G'	0.290	0.294	0.294	0.294	0.270	0.277	0.275	0.270	0.263
δ (deg.)	85.2	86.4	87.6	89.6	89.2	89.7	91.3	94.4	90.4
χ^2	2.0	2.8	2.7	3.1	2.4	3.2	3.2	3.4	2.5

Table 2: Fitted parameters for different cases of interest.

Table 2 together with the χ^2 values. It is clear that the fits are good and that the parameters are stable against variation of the branching ratio. The predicted background phase is seen to be close to 90° in both cases. Note that the fitted width of the $f_0(980)$ is near the low end of the experimental range. The low lying sigma has a mass of around $560 MeV$ and a width of about $370 MeV$. As explained in section 3, we are not using exactly a conventional *Breit-Wigner* type form for this very broad resonance. The numbers characterizing it do however seem reasonably consistent with other determinations [5, 12, 13].

4.3 Effect of the next group of resonances

Going up in energy we encounter $J^{PC} = 2^{++}, 0^{++}$ and 1^{--} resonances in the $1300 MeV$ region. The properties of the 2^{++} state $f_2(1270)$ are very well established. For the others there is more uncertainty but the PDG lists the $f_0(1300)$ and $\rho(1450)$ as established states. However the mass of the $f_0(1300)$ can apparently lie anywhere in the $1000 - 1500 MeV$ range. In Ref. [4] it was noted that the contributions of these *next group* particles tended to cancel among themselves. Thus we do not expect their inclusion to significantly change the previous results in the range of interest up to about $1.2 GeV$.

In Fig. 5 we display the contribution of the *next group* particles by themselves to R_0^0 . (The amplitudes are summarized in Appendix C). The dashed curve is essentially a reproduction

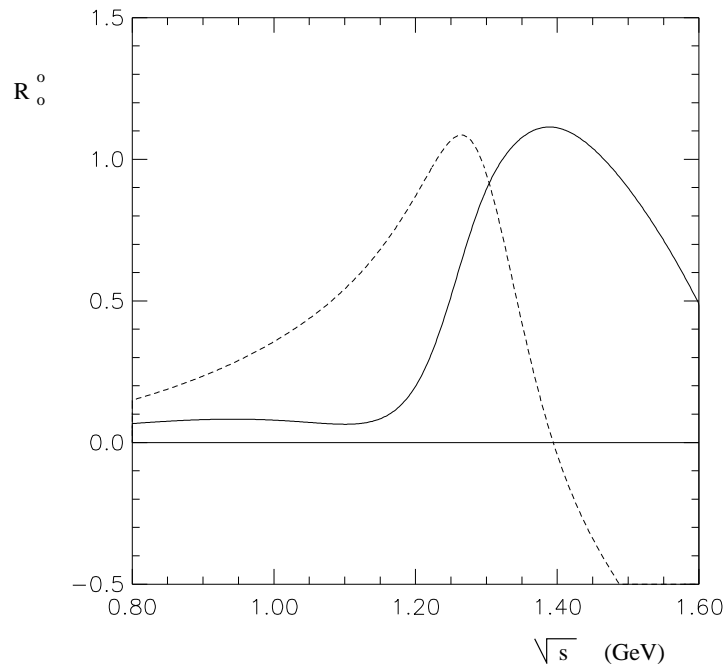


Figure 5: Contribution from the *next group* of resonances; the solid curve is obtained with the reverse sign of the $f_0(1300)$ piece.

of Fig. 6 of Ref. [4]. The somewhat positive net contribution of these resonances to R_0^0 is compensated by readjustment of the parameters describing the low lying sigma. It may be interesting to include the effect of the background phase for the $f_0(1300)$ as we have just seen that it was very important for the proper understanding of the $f_0(980)$. To test this possibility we reversed the sign of the $f_0(1300)$ contribution and show the result as the solid curve in Fig. 5. This sign reversal is reasonable since our model suggests a background phase of about 270° in the vicinity of the $f_0(1300)$. It can be seen that there is now a significantly greater cancellation of the *next group* particles among themselves up to about 1.2 GeV . The resulting total fits are shown in Fig. 6 for both 100% and 78.1% assumed $f_0(980) \rightarrow \pi\pi$ branching ratios and the parameters associated with the fits are shown in Table 2. It is clear that the fitted parameters and results up to about 1.2 GeV are very similar to the cases when the *next group* was absent. Above this region, there is now, however, a positive bump in R_0^0 at around 1.3 GeV . This could be pushed further up by choosing a higher mass (within the allowable experimental range) for the $f_0(1300)$. Resonances in the 1500 MeV region, which have *not* been taken into account here, would presumably also have an important effect in

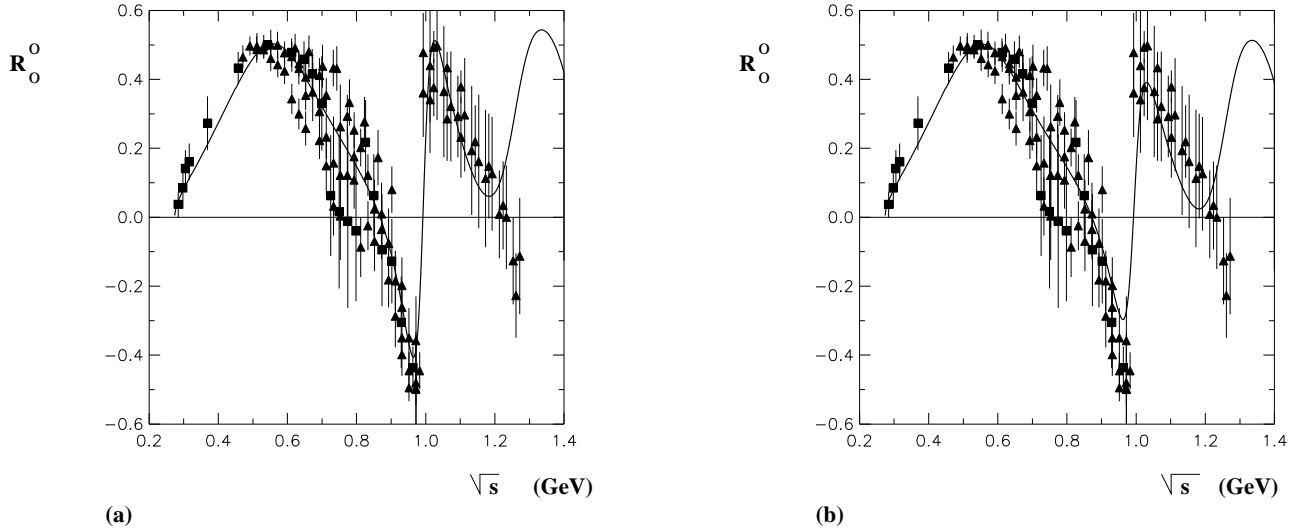


Figure 6: Prediction for R_0^0 with the *next group* of resonances. (a) assumes (column 5 in Table 2) ($BR(f_0(980) \rightarrow 2\pi) = 100\%$) while (b) assumes (column 6) ($BR(f_0(980) \rightarrow 2\pi) = 78.1\%$).

the region above 1.2 GeV . Clearly, there is not much sense, at the present stage, in trying to produce a fit above 1.2 GeV .

The analysis above assumed that the $\rho(1450)$ decays predominantly into two pions since the PDG listing does not give any specific numbers. On the other hand the $K^*(1410)$, which presumably is in the same $SU(3)$ multiplet as the $\rho(1450)$, has only a 7% branching ratio into $K\pi$. Thus it is possible that $\rho(1450)$ actually has a small coupling to $\pi\pi$. To test this out we redid the calculation with the complete neglect of the $\rho(1450)$ contribution. The resulting fit is shown in the last column of Table 2 and it is seen to leave the other parameters essentially unchanged.

It thus seems that the results are consistent with the hypothesis of *local cancellation*, wherein the physics up to a certain energy E is described by including only those resonances up to slightly more than E and it is furthermore hypothesized that the individual particles cancel in such a way that unitarity is maintained.

4.4 Effects of inelasticity

Up to now we have completely neglected the effects of coupled inelastic channels. Of course the 4π channel opens at 540 MeV , the 6π channel opens at 810 MeV and, probably most significantly, the $K\bar{K}$ channel opens at 990 MeV . We have seen that a nice understanding of the $\pi\pi$ elastic channel up to about 1.2 GeV can be gotten with complete disregard of inelastic effects. Nevertheless it is interesting to see how our results would change if experimental data on the elasticity parameter η_0^0 are folded into the analysis. Figure 7 illustrates the results for

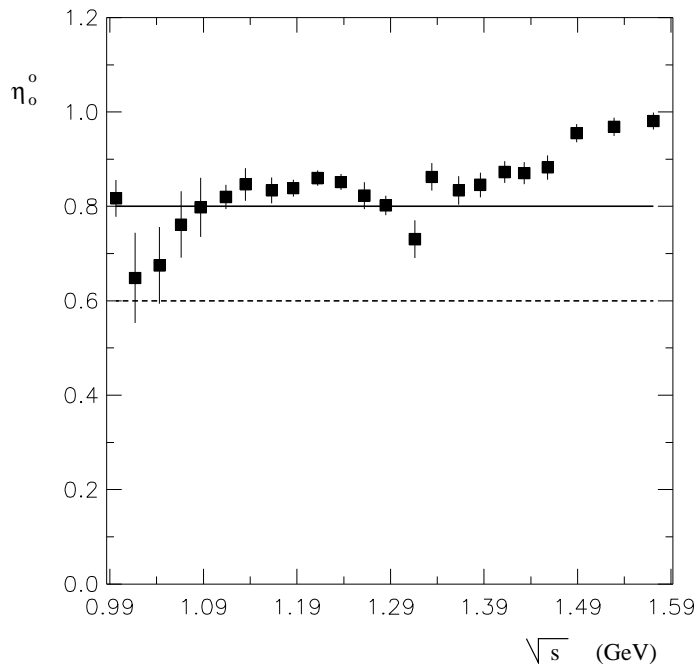


Figure 7: An experimental determination of $\eta_0^0 = \sqrt{1 - 4|T_{12,0}^0|^2}$ [14].

$\eta_0^0(s)$ obtained from an experimental analysis [14] of $\pi\pi \rightarrow K\bar{K}$ scattering. For simplicity, we approximated the data by a constant value $\eta_0^0 = 0.8$ above the $K\bar{K}$ threshold. Figure 8(a) shows the effect of this choice on $R_0^0(s)$ computed without the inclusion of the *next group* of resonances, while Fig. 8(b) shows the effect when the *next group* is included. Comparing with Fig. 4(b) and 6(b), we see that setting $\eta_0^0 = 0.8$ has not made any substantial change. The parameters of the fit are shown in Table 2 as are the parameters for an alternative fit with $\eta_0^0 = 0.6$. The latter choice leads to a worse fit for R_0^0 .

We conclude that inelastic effects are not very important for understanding the main

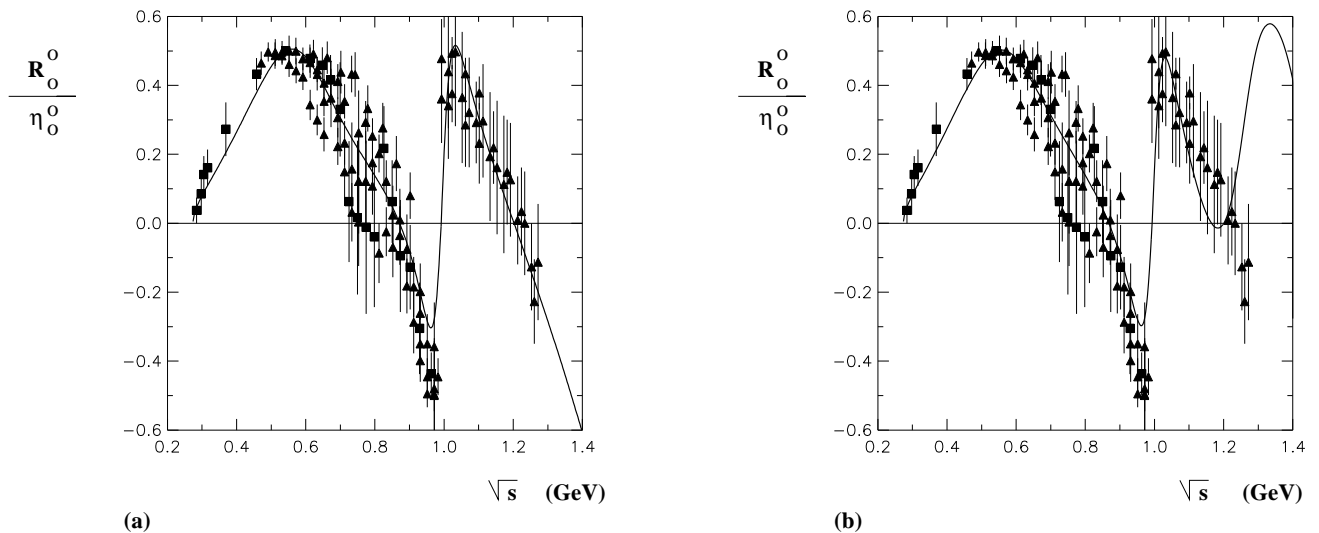


Figure 8: Predictions with phenomenological treatment of inelasticity ($\eta_0^0 = 0.8$) above $K\bar{K}$ threshold. (a): without *next group*. (b): with *next group*.

features of $\pi\pi$ scattering up to about 1.2 GeV . However, we will discuss the calculation of $\eta_0^0(s)$ from our model in section 5.

4.5 Phase shift

Strictly speaking our initial assumption only entitles us to compare, as we have already done, the real part of the predicted amplitude with the real part of the amplitude deduced from experiment. Since the predicted $R_0^0(s)$ up to 1.2 GeV satisfies the unitarity bound (within the fitting error) we can calculate the imaginary part $I_0^0(s)$, and hence the phase shift $\delta_0^0(s)$ on the assumption that full unitarity holds. This is implemented by substituting $R_0^0(s)$ into eq. (2.5) and resolving the discrete sign ambiguities by demanding that $\delta_0^0(s)$ be continuous and monotonically increasing (to agree with experiment). It is also necessary to know $\eta_0^0(s)$ for this purpose; we will be content with the approximations above which seem sufficient for understanding the main features of $\pi\pi$ scattering up to 1.2 GeV .

In this procedure there is a practical subtlety already discussed at the end of section IV of Ref. [4]. In order for $\delta_0^0(s)$ to increase monotonically it is necessary that the sign in front of the square root in eq. (2.5) change. This can lead to a discontinuity unless $2|R_0^0(s)|$ precisely reaches $\eta_0^0(s)$. However the phase shift is rather sensitive to small deviations from

this exact matching. Since the fitting procedure does not enforce that $|R_0^0(s)|$ go precisely to $\eta_0^0(s)/2 \approx 0.5$, this results in some small discontinuities. (These could be avoided by trying to fit the phase shift directly.)

Figure 9 shows the phase shift $\delta_0^0(s)$ estimated in this manner for parameters in the first

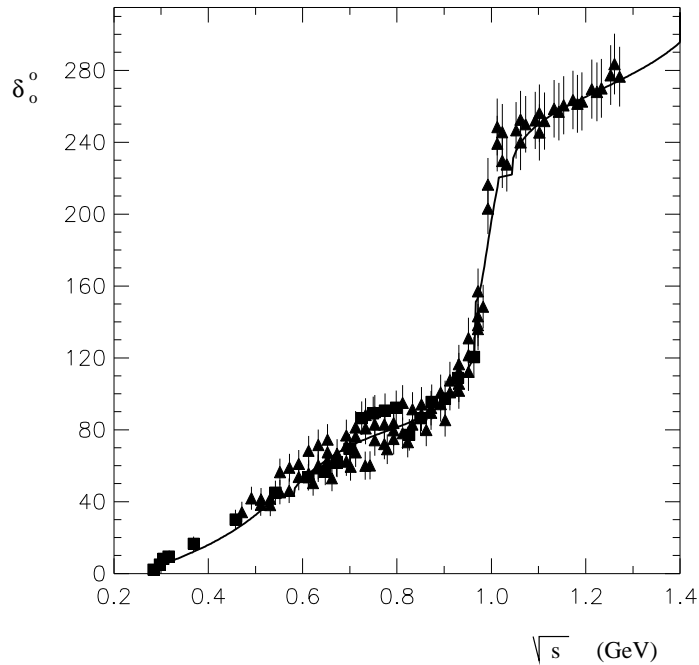


Figure 9: Estimated phase shift using the predicted real part and unitarity relation.

column of Table 2. As expected, the agreement is reasonable. A very similar estimate is obtained when (column 3 of Table 2) η_0^0 is taken to be 0.8 while considering the $\pi\pi$ branching ratio of $f_0(980)$ to be its experimental value of 78.1%. It appears that these two parameter changes are compensating each other so that one may again conclude that the turning on of the $K\bar{K}$ channel really does not have a major effect. When the *next group* of resonances is included (column 7 of Table 2) the estimated $\delta_0^0(s)$ is very similar up to about 1.2 GeV. Beyond this point it is actually somewhat worse, as we would expect by comparing Fig. 8(b) with Fig. 8(a).

5 $\pi\pi \rightarrow K\bar{K}$ Channel

We have seen that $\pi\pi \rightarrow \pi\pi$ scattering can be understood up to about 1.2 GeV with the neglect of this inelastic channel. In particular, a phenomenological description of the inelasticity did not change the overall picture. However we would like to begin to explore the predictions of the present model for this channel also. The whole coupled channel problem is a very complicated one so we will be satisfied here to check that the procedure followed for the $\pi\pi$ elastic channel can lead to an inelastic amplitude which also satisfies the unitarity bounds. Specifically we will confine our attention to the real part of the $I = J = 0$ $\pi\pi \rightarrow K\bar{K}$ amplitude, $R_{12;0}^0$ defined in eq. (A.11).

In exact analogy to the $\pi\pi \rightarrow \pi\pi$ case we first consider the contribution of the contact plus the $K^*(892)$ plus the $\sigma(550)$ terms. It is necessary to know the coupling strength of the σ to $K\bar{K}$, defined by the effective Lagrangian piece

$$-\frac{\gamma_{\sigma K\bar{K}}}{2}\sigma\partial_\mu\bar{K}\partial_\mu K. \quad (5.1)$$

If the σ is ideally mixed and there is no OZI rule violating piece we would have $\gamma_{\sigma K\bar{K}} = \gamma_0$ as defined in eq. (B.11). For definiteness, we shall adopt this standard mixing assumption. The appropriate amplitudes are listed in Appendix C. Figure 10 shows the plots of $R_{12;0}^0$ for the current algebra part alone, the current algebra plus K^* and the current algebra plus K^* plus σ parts. Notice that unitarity requires

$$|R_{12;0}^0| \leq \frac{\sqrt{1 - \eta_0^2}}{2} \leq \frac{1}{2}. \quad (5.2)$$

The current algebra result already clearly violates this bound at 1.05 GeV . As before, this is improved by the K^* vector meson exchange contribution and further improved by the very important tail of the σ contribution. The sum of all three shows a structure similar to the corresponding Fig. 2 in the $\pi\pi \rightarrow \pi\pi$ case. The unitarity bound is not violated until about 1.55 GeV .

Next, let us consider the contribution of the $f_0(980)$ which, since the resonance straddles the threshold, is expected to be important. We need to know the effective coupling constant of the f_0 to $\pi\pi$ and to $K\bar{K}$. As we saw in eq. (4.4), and the subsequent discussion, the

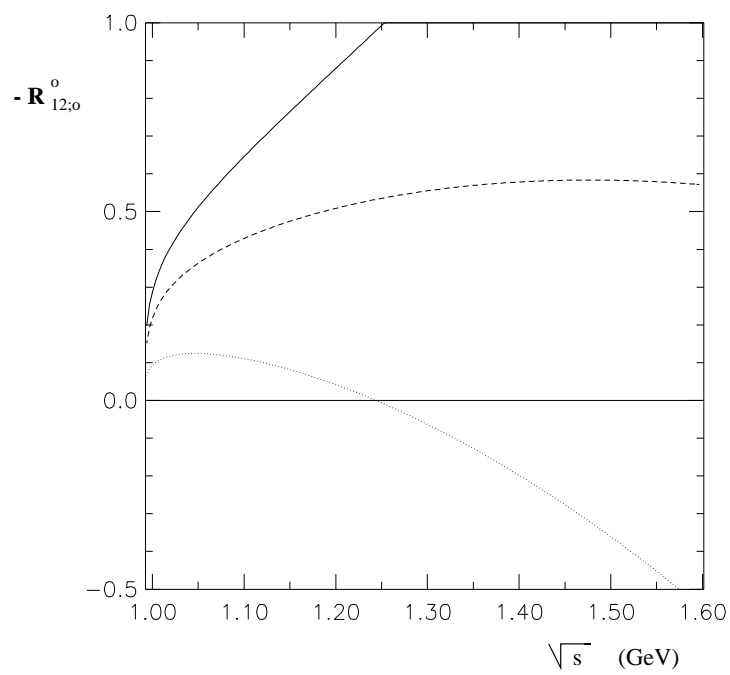


Figure 10: Contributions to $\pi\pi \rightarrow K\bar{K}$ ($R_{12;0}^0$). The solid line shows the current algebra result; the dashed line represents the inclusion of $K^*(892)$; the dotted line includes the $\sigma(550)$ too.

effective $\pi\pi$ coupling should be taken as $\gamma_{f_0\pi\pi}e^{i\frac{\pi}{2}}$. Experimentally, only the branching ratios for $f_0(980) \rightarrow \pi\pi$ and $f_0(980) \rightarrow K\bar{K}$ are accurately known. We will adopt for definiteness the value of $\gamma_{f_0\pi\pi}$ corresponding to the fit in the third column of Table 2 ($\Gamma_{tot}(f_0(980)) = 76 \text{ MeV}$). It is more difficult to estimate the $f_0(980) \rightarrow K\bar{K}$ effective coupling constant since the central value of the resonance may actually lie *below* the threshold. By taking account ¶ of the finite width of the $f_0(980)$ we get the rough estimate $|\gamma_{f_0K\bar{K}}| = 10 \text{ GeV}^{-1} \approx 4|\gamma_{f_0\pi\pi}|$ for the choice in the third column, $M_{f_0(980)} = 990 \text{ MeV}$. Of course, this estimate is very sensitive to the exact value used for $M_{f_0(980)}$. It seems reasonable to take $\gamma_{f_0K\bar{K}}$ to be purely real. The results of including the $f_0(980)$ contribution, for both sign choices of $\gamma_{f_0K\bar{K}}$, are shown in Fig. 11. The unitarity bounds are satisfied for the positive sign of $\gamma_{f_0K\bar{K}}$ but slightly violated for the negative sign choice.

Finally, let us consider the contributions to $\pi\pi \rightarrow K\bar{K}$ from the members of the multiplets containing the *next group* of particles. There will be a crossed channel contribution from the strange excited vector meson $K^*(1410)$. However it will be very small since $K^*(1410)$ predominately couples to $K^*\pi$ and has only a 7% branching ratio to $K\pi$. In addition there will be a crossed channel scalar $K_0^*(1430)$ diagram as well as a direct channel scalar $f_0(1300)$ diagram contributing to $\pi\pi \rightarrow K\bar{K}$. The $f_0(1300)$ piece is small because $f_0(1300)$ has a very small branching ratio to $K\bar{K}$. Furthermore the $K_0^*(1430)$ piece turns out also to be small; we have seen that the crossed channel scalar gave a negligible contribution to $\pi\pi \rightarrow \pi\pi$. The dominant *next group* diagrams involve the tensor mesons. Near threshold, the crossed channel $K_2^*(1430)$ diagram is the essential one since the direct channel $f_2(1270)$ contribution for the $J = 0$ partial wave is suppressed by a spin-2 projection operator. Above 1270 MeV

¶With $\Gamma_{tot}(f_0(980)) = 76 \text{ MeV}$ we would have $\Gamma(f_0(980) \rightarrow K\bar{K}) = 16.6 \text{ MeV}$. Then $\gamma_{f_0K\bar{K}}$ is estimated from the formula:

$$16.6 \text{ MeV} = |\gamma_{f_0K\bar{K}}|^2 \int_{2m_K}^{\infty} \rho(M) |A(f_0(M) \rightarrow K\bar{K})|^2 \Phi(M) dM ,$$

where $A(f_0(M) \rightarrow K\bar{K})$ is the reduced amplitude for an f_0 of mass M to decay to $K\bar{K}$, $\Phi(M)$ is the phase space factor and $\rho(M)$ is the weighting function given by

$$\rho(M) = \sqrt{\frac{2}{\pi}} \frac{1}{\Gamma_{tot}} \exp \left\{ -2 \left[\frac{(M - M_0)^2}{\Gamma_{tot}^2} \right] \right\} .$$

Here, M_0 is the central mass value of the $f_0(980)$.

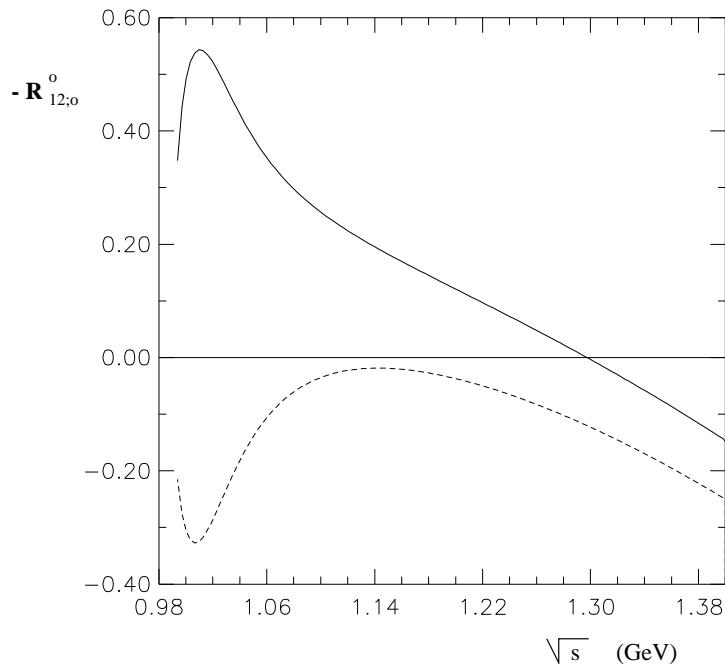


Figure 11: Effect of $f_0(980)$ on $\pi\pi \rightarrow K\bar{K}$. The solid curve corresponds to a negative $\gamma_{f_0K\bar{K}}$ and the dashed one to a positive sign.

the $f_2(1270)$ contribution becomes increasingly important although it has the opposite sign to the crossed channel tensor piece. Figure 12 shows the net prediction for $R_{12;0}^0$ obtained with the inclusion of the main *next group* contributions from the $K_2^*(1430)$ and $f_2(1270)$. Both assumed signs for $\gamma_{f_0K\bar{K}}$ are shown and other parameters correspond to column 3 of Table 2. Clearly there is an appreciable effect. Figure 13 shows the magnitude of $|R_{12;0}^0|$ together with one experimental determination [14] of $|T_{12;0}^0| = \sqrt{(R_{12;0}^0)^2 + (I_{12;0}^0)^2}$. The positive sign of $\gamma_{f_0K\bar{K}}$ is favored but, considering the uncertainty in $|\gamma_{f_0K\bar{K}}|$ among other things, we shall not insist on this. It seems to us that the main conclusion is that the unitarity bound can be satisfied in the energy range of interest.

6 Summary and Discussion

We have obtained a simple approximate analytic form for the real part of the $\pi\pi$ scattering amplitude in the energy range from threshold to about 1.2 GeV . It satisfies both crossing symmetry and (more non-trivially) unitarity in this range. Inspired by the leading $1/N_c$

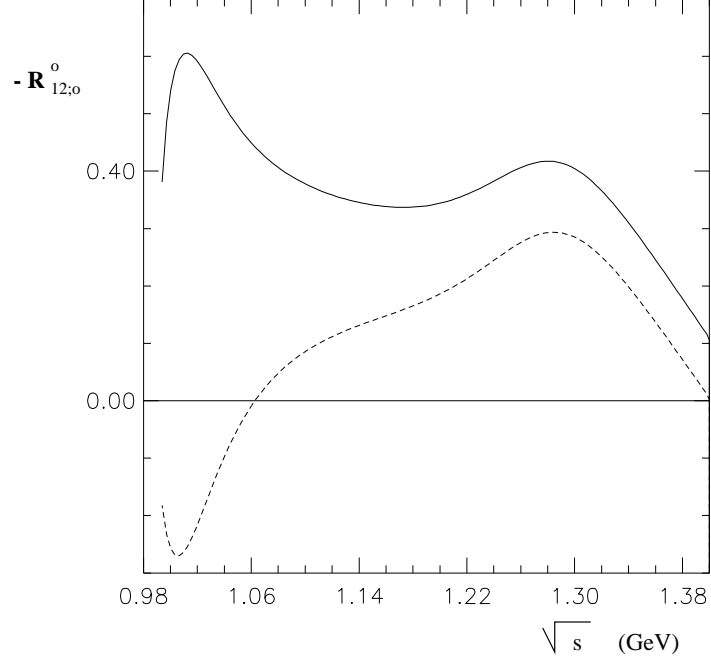


Figure 12: Effects on $\pi\pi \rightarrow K\bar{K}$ due to the *next group* of resonances for the two different sign choices in Fig. 11.

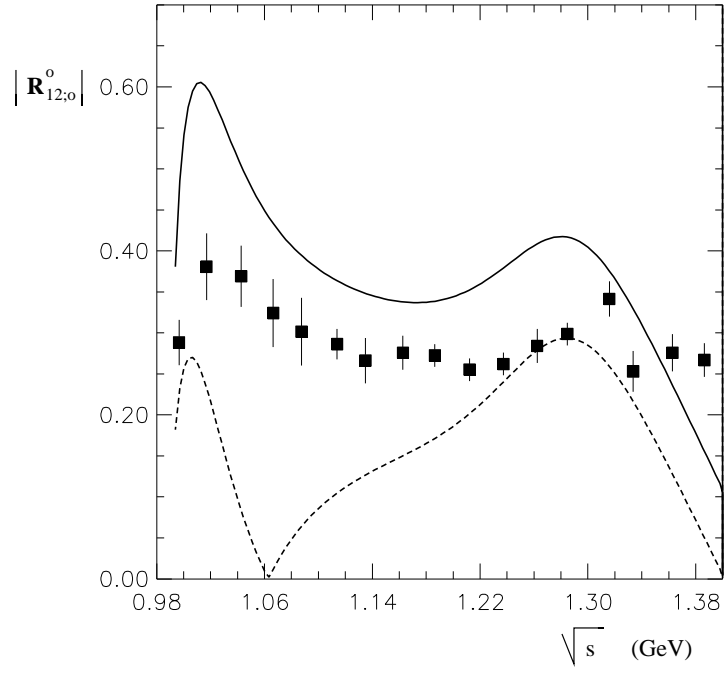


Figure 13: $|R_{12;0}^0|$ together with one experimental determination [14] of $|T_{12;0}^0| = \sqrt{(R_{12;0}^0)^2 + (I_{12;0}^0)^2}$. Signs for $\gamma_{f_0 K\bar{K}}$ as in Fig. 11

approximation, we have written the amplitude as the sum of a contact term and poles. Of course the leading $1/N_c$ amplitude can not be directly compared with experiment since it is purely real (away from the direct channel poles) and diverges at the pole positions. Furthermore, an infinite number of poles, and higher derivative interactions are in principle needed. To overcome these problems we have employed the following procedure.

- a. We specialized to predicting the real part of the amplitude.
- b. We postulated that including only resonances from threshold to slightly more than the maximum energy of interest is sufficient. We have seen that this *local cancellation* appears stable under the addition of resonances in the 1300 *MeV* range. Beyond this range we would expect still higher resonances to add in such a way so as to enforce unitarity at still higher energies.
- c. In the effective interaction Lagrangian we included only terms with the minimal number of derivatives consistent with the assumed chiral symmetry.
- d. The most subtle aspect concerns the method for regularizing the divergences at the direct channel resonance poles. In the simplest case of a single resonance dominating a particular channel (e.g. the ρ meson) it is sufficient to add the standard *width* term to the denominator (e.g. the real part of eq. (2.2)). For an extremely broad resonance (like a needed low energy scalar isosinglet) the concept of *width* is not so clear and we employed the slight modification of the Breit-Wigner amplitude given in eq. (2.3). Finally, for a relatively narrow resonance in the presence of a non-negligible background we employed the regularization given in eq. (2.4) which includes the background phase. Self-consistency is assured by requiring that the background phase should be predicted by the model itself.

All the regularizations introduced above are formally of higher than leading order in the $1/N_c$ expansion (i.e. of order $1/N_c^2$ and higher) and correspond physically to rescattering effects. In the case of non-negligible background phase, there is an interesting difference from the usual tree-level treatment of pole diagrams. The effective squared coupling constant, $g_{R\pi\pi}^2$ of such a resonance to two pions, is then not necessarily real positive. Since this

regularization is interpreted as a rescattering effect it does not mean that ghost fields are present in the theory. This formulation maintains crossing symmetry which is typically lost when a unitarization method is employed.

In this analysis, the most non-trivial point is the satisfaction of the unitarity bound for the predicted real part of the partial wave amplitude,

$$|R_l^I| \leq \frac{\eta_l^I}{2}, \quad (6.1)$$

where $\eta_l^I < 1$ is the elasticity parameter. The well known difficulty concerns R_0^0 . If $\eta_l^I(s)$ is known or calculated the imaginary part $I_l^I(s)$ can be obtained, up to discrete ambiguities, by eq. (2.5).

The picture of $\pi\pi$ scattering in the threshold to slightly more than 1 GeV range which emerges from this model has four parts. Very near threshold the current algebra contact term approximates $R_0^0(s)$ very well. The imaginary part $I_0^0(s)$, which is formally of order $1/N_c^2$ can be obtained from unitarity directly using eq. (2.5) or, equivalently, by chiral perturbation theory. At somewhat higher energies the most prominent feature is the ρ meson pole in the $I = J = 1$ channel. The crossed channel ρ exchange is also extremely important in taming the elastic unitarity violation associated with the current algebra contact term (Fig. 1). Even with the ρ present, Fig. 1 shows that unitarity is still violated, though much less drastically. This problem is overcome by introducing a low mass $\approx 550 MeV$, extremely broad sigma meson. It also has another desirable feature: $R_0^0(s)$ is boosted (see Fig. 3) closer to experiment in the 400–500 MeV range. The three parameters characterizing this particle are essentially the only unknowns in the model and were determined by making a best fit. In the 1 GeV region it seems clear that the $f_0(980)$ resonance, interacting with the predicted background in the manner of the *Ramsauer-Townsend* effect, dominates the structure of the $I = J = 0$ phase shift. The inelasticity associated with the opening of the $K\bar{K}$ threshold has a relatively small effect. However we also presented a preliminary calculation which shows that the present approach satisfies the unitarity bounds in the inelastic $\pi\pi \rightarrow K\bar{K}$ channel.

Other recent works [5, 12, 13, 15, 16] which approach the problem in different ways, also contain a low mass broad sigma. The question of whether the lighter scalar mesons are of $q\bar{q}$ type or *meson-meson* type has also been discussed [5, 12, 13]. In our model it

is difficult to decide this issue. Of course, it is not a clean question from a field theoretic standpoint. This question is important for understanding whether the contributions of such resonances are formally leading in the $1/N_c$ expansion. We are postponing the answer as well as the answer to how to derive the rescattering effects that were used to *regularize* the amplitude near the direct channel poles as higher order in $1/N_c$ corrections. Presumably, the rescattering effects could some day be calculated as loop corrections with a (very complicated) effective Wilsonian action. This would be a generalization of the chiral perturbation scheme of pions. Another aspect of the $1/N_c$ picture concerns the infinite number of resonances which are expected to contribute already at leading order. One may hope that the idea of *local cancellation* will help in the development of a simple picture at high energies which might get patched together with the present one. Is the simple high energy theory a kind of string model ?

From a practical standpoint (without worrying about all the theoretical issues involved in making a comparison with the $1/N_c$ expansion) we have demonstrated that it is possible to understand $\pi\pi$ scattering up to the 1 GeV region by shoehorning together poles and contact term contributions employing a suitable regularization procedure. It seems likely that any crossing symmetric approximation will have a similar form. This is in the spirit of *mean field* theories.

Acknowledgments

This work was supported in part by the U.S. DOE Contract No. DE-FG-02-85ER40231.

Appendix A

Scattering kinematics

The general partial wave scattering matrix for the multi channel case can be written as:

$$S_{ab} = \delta_{ab} + 2iT_{ab} . \quad (\text{A.1})$$

For simplicity, the diagonal isospin and angular momentum labels have not been indicated.

By requiring the unitarity condition $S^\dagger S = 1$ one deduces for the two channel case the following relations:

$$\begin{aligned} \text{Im}(T_{11}) &= |T_{11}|^2 + |T_{21}|^2 , \\ \text{Im}(T_{22}) &= |T_{22}|^2 + |T_{12}|^2 , \\ \text{Im}(T_{12}) &= T_{11}^* T_{12} + T_{12}^* T_{22} , \end{aligned} \quad (\text{A.2})$$

where $T_{12} = T_{21}$. In the present case we will identify 1 as the $\pi\pi$ channel and 2 as the $K\bar{K}$ channel. In order to get the relations between the relative phase shifts and the amplitude we need to consider the following parameterization of the scattering amplitude:

$$S = \begin{pmatrix} \eta e^{2i\delta_\pi} & \pm i\sqrt{1-\eta^2} e^{i\delta_{\pi K}} \\ \pm i\sqrt{1-\eta^2} e^{i\delta_{\pi K}} & \eta e^{2i\delta_K} \end{pmatrix} , \quad (\text{A.3})$$

where $\delta_{\pi K} = \delta_\pi + \delta_K$ and $0 < \eta < 1$ is the elasticity parameter. By comparing eq. (A.3) and eq. (A.1) one can easily deduce:

$$\eta^2 = 1 - 4|T_{12}|^2 . \quad (\text{A.4})$$

Analogously, for T_{aa} we have:

$$T_{aa;l}^I(s) = \frac{(\eta_l^I(s) e^{2i\delta_{a;l}^I(s)} - 1)}{2i} , \quad (\text{A.5})$$

where l and I label the angular momentum and isospin, respectively. Extracting the real and imaginary parts via

$$\begin{aligned} R_{aa;l}^I &= \frac{\eta_l^I \sin(2\delta_{a;l}^I)}{2} , \\ I_{aa;l}^I &= \frac{1 - \eta_l^I \cos(2\delta_{a;l}^I)}{2} \end{aligned} \quad (\text{A.6})$$

leads to the very important bounds

$$|R_{aa;l}^I| \leq \frac{1}{2}, \quad 0 \leq I_{aa;l}^I \leq 1. \quad (\text{A.7})$$

The unitarity also requires $|T_{12;l}^I| < 1/2$.

Now we relate these partial wave amplitudes to the invariant amplitudes. The invariant amplitude for $\pi_i(p_1) + \pi_j(p_2) \rightarrow \pi_k(p_3) + \pi_l(p_4)$ is decomposed as:

$$\delta_{ij}\delta_{kl}A(s, t, u) + \delta_{ik}\delta_{jl}A(t, s, u) + \delta_{il}\delta_{jk}A(u, t, s), \quad (\text{A.8})$$

where s , t and u are the usual Mandelstam variables. Note that the phase of eq. (A.8) corresponds to simply taking the matrix element of the Lagrangian density of a four point contact interaction. Projecting out amplitudes of definite isospin yields:

$$\begin{aligned} T_{11}^0(s, t, u) &= 3A(s, t, u) + A(t, s, u) + A(u, t, s), \\ T_{11}^1(s, t, u) &= A(t, s, u) - A(u, t, s), \\ T_{11}^2(s, t, u) &= A(t, s, u) + A(u, t, s). \end{aligned} \quad (\text{A.9})$$

The needed $I = 0$ $\pi\pi \rightarrow K\bar{K}$ amplitude can be gotten as:

$$T_{12}^0(s, t, u) = -\sqrt{6}A(\pi^0(p_1)\pi^0(p_2), K^+(p_3)K^-(p_4)). \quad (\text{A.10})$$

We then define the partial wave isospin amplitudes according to the following formula:

$$T_{ab;l}^I(s) \equiv \frac{1}{2}\sqrt{\rho_a\rho_b} \int_{-1}^1 d\cos\theta P_l(\cos\theta)T_{ab}^I(s, t, u), \quad (\text{A.11})$$

where θ is the scattering angle and

$$\rho_a = \frac{1}{S} \frac{1}{16\pi} \sqrt{\frac{s - 4m_\pi^2}{s}} \theta(s - 4m_a^2). \quad (\text{A.12})$$

S is a symmetry factor which is 2 for identical particles ($\pi\pi$ case) and 1 for distinguishable particles ($K\bar{K}$ case).

Appendix B

Chiral Lagrangian

In the low energy physics of hadrons, it is important to take account of the spontaneous chiral symmetry breaking structure. We start here with the $U(3)_L \times U(3)_R / U(3)_V$ non-linear realization of chiral symmetry. The basic quantity is a 3×3 matrix U , which transforms as

$$U \rightarrow U_L U U_R^\dagger, \quad (\text{B.1})$$

where $U_{L,R} \in U(3)_{L,R}$. This U is parameterized by the pseudoscalar ϕ as

$$U = \xi^2, \quad \xi = e^{2i\phi/F_\pi}, \quad (\text{B.2})$$

where F_π is a pion decay constant. Under the chiral transformation eq. (B.1), ξ transforms non-linearly:

$$\xi \rightarrow U_L \xi K^\dagger(\phi, U_L, U_R) = K(\phi, U_L, U_R) \xi U_R^\dagger. \quad (\text{B.3})$$

The vector meson nonet ρ_μ is introduced as a *gauge field* [17] which transforms as

$$\rho_\mu \rightarrow K \rho_\mu K^\dagger + \frac{i}{\tilde{g}} K \partial_\mu K^\dagger, \quad (\text{B.4})$$

where \tilde{g} is a *gauge coupling constant*. (For an alternative approach see, for a review, Ref. [18].)

It is convenient to define

$$\begin{aligned} p_\mu &= \frac{i}{2} \left(\xi \partial_\mu \xi^\dagger - \xi^\dagger \partial_\mu \xi \right), \\ v_\mu &= \frac{i}{2} \left(\xi \partial_\mu \xi^\dagger + \xi^\dagger \partial_\mu \xi \right), \end{aligned} \quad (\text{B.5})$$

which transform as

$$\begin{aligned} p_\mu &\rightarrow K p_\mu K^\dagger, \\ v_\mu &\rightarrow K v_\mu K^\dagger + i K \partial_\mu K^\dagger. \end{aligned} \quad (\text{B.6})$$

Using the above quantities we construct the chiral Lagrangian including both pseudoscalar and vector mesons:

$$\mathcal{L} = -\frac{1}{2} m_v^2 \text{Tr} [(\tilde{g} \rho_\mu - v_\mu)^2] - \frac{F_\pi^2}{2} \text{Tr} [p_\mu p_\mu] - \frac{1}{4} \text{Tr} [F_{\mu\nu}(\rho) F_{\mu\nu}(\rho)], \quad (\text{B.7})$$

where $F_{\mu\nu} = \partial_\mu\rho_\nu - \partial_\nu\rho_\mu - i\tilde{g}[\rho_\mu, \rho_\nu]$ is a *gauge field strength* of vector mesons.

In the real world chiral symmetry is explicitly broken by the quark mass term $-\widehat{m}\bar{q}\mathcal{M}q$, where $\widehat{m} \equiv (m_u + m_d)/2$, and \mathcal{M} is the dimension-less matrix:

$$\mathcal{M} = \begin{pmatrix} 1 + y & & \\ & 1 - y & \\ & & x \end{pmatrix}. \quad (\text{B.8})$$

Here x and y are the quark mass ratios:

$$x = \frac{m_s}{\widehat{m}}, \quad y = \frac{1}{2} \left(\frac{m_d - m_u}{\widehat{m}} \right). \quad (\text{B.9})$$

These quark masses lead to mass terms for pseudoscalar mesons. Moreover, in considering the processes related to the kaon, (in this paper we will consider $\pi\pi \rightarrow K\bar{K}$ scattering amplitude.) we need to take account of the large splitting of the s quark mass from the u and d quark masses. These effects are included as SU(3) symmetry breaking terms in the above Lagrangian, which are summarized, for example, in Refs. [19, 20]. Here we write the lowest order pseudoscalar mass term only:

$$\mathcal{L}_{\phi\text{-mass}} = \delta' \text{Tr} \left[\mathcal{M}U^\dagger + \mathcal{M}^\dagger U \right], \quad (\text{B.10})$$

where δ' is an arbitrary constant.

We next introduce higher resonances into our Lagrangian. First, we write the interaction between the scalar nonet field S and pseudoscalar mesons. Under the chiral transformation, this S transforms as $S \rightarrow KSK^\dagger$. A possible form which includes the minimum number of derivatives is proportional to $\text{Tr} [Sp_\mu p_\mu]$. The coupling of a physical isosinglet field to two pions is then described by

$$\mathcal{L}_\sigma = -\frac{\gamma_0}{\sqrt{2}} \sigma \partial_\mu \vec{\pi} \cdot \partial_\mu \vec{\pi}. \quad (\text{B.11})$$

Here we should note that the chiral symmetry requires derivative-type interactions between scalar fields and pseudoscalar mesons. Second, we represent the tensor nonet field by $T_{\mu\nu}$ (satisfying $T_{\mu\nu} = T_{\nu\mu}$, and $T_{\mu\mu} = 0$), which transforms as $T_{\mu\nu} \rightarrow KT_{\mu\nu}K^\dagger$. The interaction term is given by

$$\mathcal{L}_T = -\gamma_2 F_\pi^2 \text{Tr} [T_{\mu\nu} p_\mu p_\nu]. \quad (\text{B.12})$$

The heavier vector resonances such as $\rho(1450)$ can be introduced in the same way as ρ in eq. (B.7).

Appendix C

Unregularized amplitudes

Amplitudes for the $\pi\pi \rightarrow \pi\pi$ channel

The current algebra contribution to $A(s, t, u)$ is

$$A_{ca}(s, t, u) = 2 \frac{(s - m_\pi^2)}{F_\pi^2} . \quad (\text{C.1})$$

The amplitude for the vectors can be expressed in the following form

$$A_\rho(s, t, u) = -\frac{g_{\rho\pi\pi}^2}{2m_\rho^2} \left[\frac{t(u-s)}{m_\rho^2 - t} + \frac{u(t-s)}{m_\rho^2 - u} \right] , \quad (\text{C.2})$$

where $g_{\rho\pi\pi}$ is the coupling of the vector to two pions.

For the scalar particle we deduce

$$A_{f_0}(s, t, u) = \frac{\gamma_0^2 (s - 2m_\pi^2)^2}{2 m_{f_0}^2 - s} . \quad (\text{C.3})$$

To calculate the tensor exchange diagram we need the spin 2 propagator [21]

$$\frac{-i}{m_{f_2}^2 + q^2} \left[\frac{1}{2} (\theta_{\mu_1\nu_1}\theta_{\mu_2\nu_2} + \theta_{\mu_1\nu_2}\theta_{\mu_2\nu_1}) - \frac{1}{3}\theta_{\mu_1\mu_2}\theta_{\nu_1\nu_2} \right] , \quad (\text{C.4})$$

where

$$\theta_{\mu\nu} = \delta_{\mu\nu} + \frac{q_\mu q_\nu}{m_{f_2}^2} . \quad (\text{C.5})$$

A straightforward computation then yields the f_2 contribution to the $\pi\pi$ scattering amplitude:

$$A_{f_2}(s, t, u) = \frac{\gamma_2^2}{2(m_{f_2}^2 - s)} \left(-\frac{16}{3}m_\pi^4 + \frac{10}{3}m_\pi^2 s - \frac{1}{3}s^2 + \frac{1}{2}(t^2 + u^2) - \frac{2}{3}\frac{m_\pi^2 s^2}{m_{f_2}^2} - \frac{s^3}{6m_{f_2}^2} + \frac{s^4}{6m_{f_2}^4} \right) . \quad (\text{C.6})$$

Amplitudes for $\pi^0\pi^0 \rightarrow K^+K^-$

Current algebra amplitude:

$$A_{ca}(\pi^0\pi^0, K^+K^-) = \frac{s}{2F_\pi^2} . \quad (\text{C.7})$$

Vector meson contribution:

$$\begin{aligned}
A_{Vector}(\pi^0\pi^0, K^+K^-) &= \frac{g_{K^*K\pi}^2}{8m_{K^*}^2} \left[\frac{t(s-u)}{m_{K^*}^2 - t} + \frac{u(s-t)}{m_{K^*}^2 - u} \right. \\
&\quad \left. + (m_k^2 - m_\pi^2)^2 \left(\frac{1}{m_{K^*}^2 - t} + \frac{1}{m_{K^*}^2 - u} \right) \right]. \quad (C.8)
\end{aligned}$$

Direct channel contribution for the scalar:

$$A_{f_0}(\pi^0\pi^0, K^+K^-) = \frac{1}{4} \gamma_{f_0\pi\pi} \gamma_{f_0K\bar{K}} \frac{(s - 2m_\pi^2)(s - 2m_k^2)}{m_{f_0}^2 - s}. \quad (C.9)$$

Cross channel contribution for the scalar:

$$A_{K_0^*}(\pi^0\pi^0, K^+K^-) = \frac{\gamma_{K_0^*K\pi}^2}{8} \left[\frac{(m_K^2 + m_\pi^2 - t)^2}{m_{K_0^*}^2 - t} + \frac{(m_K^2 + m_\pi^2 - u)^2}{m_{K_0^*}^2 - u} \right]. \quad (C.10)$$

Direct channel tensor contribution:

$$\begin{aligned}
A_{f_2}(\pi^0\pi^0, K^+K^-) &= \frac{\gamma_{2\pi\pi} \gamma_{2K\bar{K}}}{2(m_{f_2}^2 - s)} \left[\left(\frac{s^2}{4m_{f_2}^2} + \frac{t}{2} - \frac{(m_\pi^2 + m_K^2)}{2} \right)^2 \right. \\
&\quad + \left(\frac{s^2}{4m_{f_2}^2} + \frac{u}{2} - \frac{(m_\pi^2 + m_K^2)}{2} \right)^2 \\
&\quad \left. - \frac{2}{3} \left(\frac{s^2}{4m_{f_2}^2} - \frac{s}{2} + m_\pi^2 \right) \left(\frac{s^2}{4m_{f_2}^2} - \frac{s}{2} + m_K^2 \right) \right]. \quad (C.11)
\end{aligned}$$

Cross channel tensor contribution:

$$\begin{aligned}
A_{K_2^*}(\pi^0\pi^0, K^+K^-) &= \frac{\gamma_{2K\pi}^2}{16(m_{K_2^*}^2 - t)} \left\{ \left[(2m_\pi^2 - s) - \frac{1}{2m_{K_2^*}^2} (m_\pi^2 - m_K^2 + t)^2 \right] \right. \\
&\quad \times \left[(2m_K^2 - s) - \frac{1}{2m_{K_2^*}^2} (m_K^2 - m_\pi^2 + t)^2 \right] \\
&\quad + \left[(u - m_\pi^2 - m_K^2) + \frac{1}{2m_{K_2^*}^2} (t^2 - (m_K^2 - m_\pi^2)^2) \right]^2 \\
&\quad \left. - \frac{2}{3} \left[(t - m_\pi^2 - m_K^2) - \frac{1}{2m_{K_2^*}^2} (t^2 - (m_K^2 - m_\pi^2)^2) \right]^2 \right\} \\
&\quad + (t \longleftrightarrow u). \quad (C.12)
\end{aligned}$$

References

- [1] S. Weinberg, *Physica* **96A**, 327 (1979). J. Gasser and H. Leutwyler, *Ann. of Phys.* **158** 142 (1984); J. Gasser and H. Leutwyler, *Nucl. Phys.* **B250** 465 (1985). A recent review is given by Ulf-G. Meißner, *Rept. Prog. Phys.* **56**, 903 (1993).
- [2] E. Witten, *Nucl. Phys.* **B160** 57 (1979). See also S. Coleman, *Aspects of Symmetry*, Cambridge University Press (1985). The original suggestion is given in G. 't Hooft, *Nucl. Phys.* **B72** 461 (1974).
- [3] Such a situation exists in the Veneziano model; G. Veneziano, *Nuovo Cim.* **57A** 190 (1968). A modern perspective is given in M.B. Green, J.H. Schwarz and E. Witten, *Superstring Theory Vol 1* Cambridge University Press (1987).
- [4] F. Sannino and J. Schechter, *Phys. Rev. D* **52**, 96 (1995).
- [5] See, for example, N.A. Törnqvist, Report **No. HU-SEFT R 1995-05**, (1995) (unpublished), hep-ph/9504372 and references therein.
- [6] J. R. Taylor, *Scattering Theory*, Krieger (1987).
- [7] Review of Particle Properties, L. Montanet *et al.*, *Phys. Rev. D* **50**, 1173 (1994).
- [8] E.A. Alekseeva *et al.*, *Soc. Phys. JETP* **55**, 591 (1982).
- [9] G. Grayer *et al.*, *Nucl. Phys.* **B75**, 189 (1974)
- [10] J. Gasser and Ulf-G. Meißner, *Phys. Lett. B* **258**, 219 (1991).
- [11] See pag. 109 of L.I. Schiff, *Quantum Mechanics* second edition 1955
- [12] G. Janssen, B.C. Pearce, K. Holinde and J. Speth, *Phys. Rev. D* **52**, 2690 (1995).
- [13] D. Morgan and M. Pennington, *Phys. Rev. D* **48**, 1185 (1993).
- [14] D. Cohen *et al.*, *Phys. Rev. D* **22**, 2595 (1980).
- [15] D. Atkinson, M. Harada and A.I. Sanda, *Phys. Rev. D* **46**, 3884 (1992).

- [16] A.A. Bolokhov, A.N. Manashov, M.V. Polyakov and V.V. Vereshagin, Phys. Rev. D **48**, 3090 (1993).
- [17] Ö. Kaymakcalan and J. Schechter, Phys. Rev. D **31**, 1109 (1985).
- [18] M. Bando, T. Kugo and K. Yamawaki, Phys. Rep. **164**, 217 (1988).
- [19] J. Schechter, A. Subbaraman, and H. Weigel, Phys. Rev. D **48**, 339 (1993).
- [20] M. Harada and J. Schechter, Syracuse University preprint **SU-4240-613**, (1995), hep-ph/9506473.
- [21] G. Wentzel, *Quantum Theory of Fields*, Interscience (1949) .